COMPDYN 2013
4th ECCOMAS Thematic Conference on
Computational Methods in Structural Dynamics and Earthquake Engineering
M. Papadrakakis, V. Papadopoulos, V. Plevris (eds.)
Kos Island, Greece, 12–14 June 2013

COMPUTATIONAL ASSESSMENT OF THE PROGRESSIVE COLLAPSE OF A FIVE STOREY STRUCTURE CONSIDERING TWO DIFFERENT BUILDING CODES

Cláudio E. M. Oliveira[1,2], Péter Z. Berke[2], Ricardo A. M. Silveira[1] and Thierry J. Massart[2]

[1] Federal University of Ouro Preto (UFOP)
Departamento of Civil Engineering –Graduate Program in Civil Engineering (PROPEC)
Campus Morro do Cruzeiro. Ouro Preto, MG. 35400-000. Brazil.
claudioernani@yahoo.com.br; ricardo@em.ufop.br

[2] Université Libre de Bruxelles (ULB)
Building Architecture and Town Planning (BATir) Department CP 194/2
Av. F. D. Roosevelt, 50, 1050, Brussels. Belgium.
pberke@batir.ulb.ac.be; thmassar@batir.ulb.ac.be

Keywords: Progressive Collapse, Structural Safety, Multiscale Analysis, Nonlinear Analysis, Eurocode, ABNT- NBR 6118.

Abstract. *The analysis and understanding of the progressive collapse of buildings plays significant role on the search for structural safety. The present work proposes the association of a corotational formulation, plasticity and a sectional degradation model for the analysis of reinforced concrete (RC) buildings designed in accordance to fib [1] and Eurocode [2] and also the Brazilian building code (ABNT - NBR 6118) [3]. The model makes use of a layered Euler/Bernoulli-based beam formulation and takes into account both nonlinear and dynamic aspects. The corotational formulation used for including geometrical nonlinearities is similar to the one proposed in [4]. The material nonlinearity is based on a one-dimensional elasto-viscoplastic model. A sudden column loss approach is considered, turning the formulation into a general one for dynamic analysis of planar RC frames. Also, by discretizing the transversal section into layers, it is possible to tackle the problem in a multiscale approach [5]. The chosen structures intentionally assume the minimum requirements for the design of multi-storey edifices that are proposed by fib [1] – Eurocode [2] and ABNT - NBR 6118 [3], being used to verify if these requirements are sufficient for enforcing structural safety and also to verify the major differences between those two building criteria concerning progressive collapse.*

1 INTRODUCTION

In the last few decades, progressive collapse (PC) has been addressed by many authors as a catastrophic nonlinear dynamic behavior of tall buildings which can lead to human and financial losses [6 - 9]. Its occurrence is connected to the redistribution of global loads after the loss of one or more key structural elements which, in turn, causes changes in the loading on the sectional level of these elements. Computational PC analysis not only tries to answer the question of whether a building will fail or not after such an initial structural damage, but may also allow the identification of parts of that building that could be reinforced or architectonically modified in order to prevent the occurrence of PC; thereby diminishes losses by keeping, as much as possible, the stability of the remaining structure. This is the reason why the identification of key elements and the quantification of the necessary structural robustness to prevent progressive collapse are subject to intensive research [10 - 12].

Considering that requirements of European and Brazilian codes for reinforced concrete structures are different, they would result for similar structures in different designs in terms of loads, sections, reinforcement schemes and, consequently, structural robustness. This work has the main purpose of comparing the PC structural response of a five storey building made of reinforced concrete, keeping the same architectural design but assuming the minimum requirements established by Eurocode [2] and ABNT - NBR 6118 [3], therefore leading to two structurally different planar frames with respect to element cross sections, reinforcement scheme and reinforcement ratio. The architectonic design of the analyzed building has been previously presented by Irribarren [5] and depicts a five-storey / eight-bay building (18x40 meters) made of reinforced concrete. The Eurocode based design was carried out using the Buildsoft commercial software, Diamonds [13]. The same building was also structurally designed on Cypecad, a software by Cype [14], in accordance with the Brazilian building code. More detailed information on these models is provided in the next section. This methodology is relevant since the obtained structures correspond to realistic designs, i.e. structures that could actually be built. The resulting designs are presented in Section 2.

The PC behavior of the above mentioned models is investigated in a multiscale approach [5], and takes into account nonlinear effects featured by the material behavior, i.e. strain rate dependent elastic-plastic behavior, under dynamic loading. Geometrically nonlinear effects (allowing for the representation of catenary effects) are here included in the multiscale framework and investigated by means of a corotational formulation [4]. The resulting numerical tool is presented in Section 3.

The obtained numerical results are compared in terms of damage extent correlated to the different structural designs. The results of the simulations and comparisons of structural designs obtained by the two different building codes are presented in Section 4 followed by the conclusions and perspectives of this work in Section 5.

2 STRUCTURAL DESIGN

This section is aimed at the description of the planar frame models used for the numerical PC analysis, with an emphasis on the loads and assumptions made during the process of structural design.

The architectural model comprises a 18 meter high office building composed of five floors. The ground floor is six meters high and each of the upper floors is three meters high. The 48 meters long facade is equally divided in eight bays and the unit depth of 6 meters. Progressive collapse is simulated by assuming the loss of the ground column located on the building's left side (Fig. 1).

Floor loads were distributed along the beams' length, in a way that the model could be analyzed as if it was a planar frame. Concrete slabs of 30 cm thickness were computed for the Eurocode based model and 13 cm thick slabs for the one based on the Brazilian building code. Live and dead loads are summarized in Tab. 1. The total load, shown in the same Table, assumes the combination of the total dead load value and 25% of the live loads, as recommended by GSA [10]. Self-weight load of beams and columns is calculated accordingly to the transversal section of the structural element, which is multiplied by the value of reinforced concrete weight density (24 kN/m^3). Analogous procedure is adopted for calculating the self-weight of the floors, i.e. multiplying transversal sectional area by the depth of the floor, and then by reinforced concrete density.

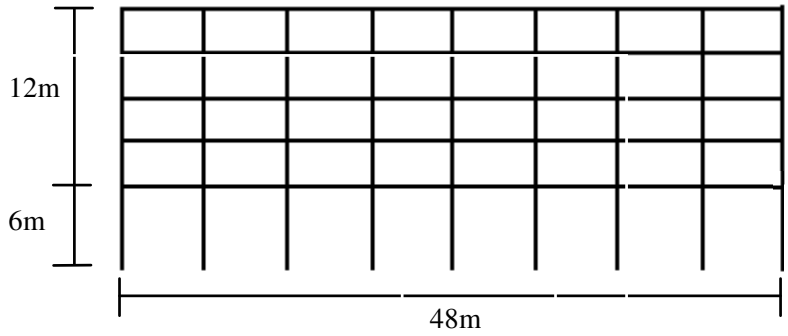

Figure 1: Architectural design [5].

	Eurocode based design			**ABNT - NBR 6118 based design**		
Loads (kN/m)	Dead	Live	Total	Dead	Live	Total
Floor Beams	43.2	18	47.7	18.7	12	21.7
Roof Beams	43.2	6	44.7	18.7	6	20.2

Table 1: Recommended beam loads.

As can be seen in Tab. 1, the value of the total loads obtained for the Brazilian reinforced concrete building code [3] is much smaller than the one obtained for Eurocode [2]. Due to this difference in the load levels, the structural analysis results in different sections of the columns and beams as well as their reinforcement schemes. In order to have a good agreement with guidelines applied in the practical construction, some requirements need to be defined before the structural designing process. These requirements are:

- all floor beams are the same, i.e. no difference regarding loads was considered from floor to floor;
- all columns are the same, i.e. although floor columns bear smaller loads, they have the same section and reinforcement scheme as ground columns;
- height and width of a structural element are constant along the length of that element;
- the concrete envelope (layer of concrete that covers steel bars) is of 5 cm and 2.5 cm for Eurocode and ABNT - NBR 6118 based designs, respectively;
- bottom reinforcements are continuous in both designs;
- both structural designs consider continuity of 2/3 of the top beam reinforcements (Fig. 2, Fig. 3) ;

Additionally, in the numerical simulations:

- Stirrups are considered during design, but not represented in input data for PC analysis.

Reinforcement schemes for both designs are shown on Figs. 2 and 3.

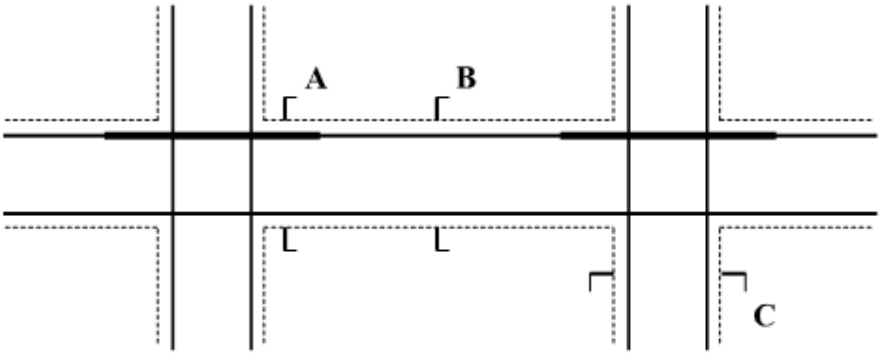

Figure 2: Reinforcement continuity [5].

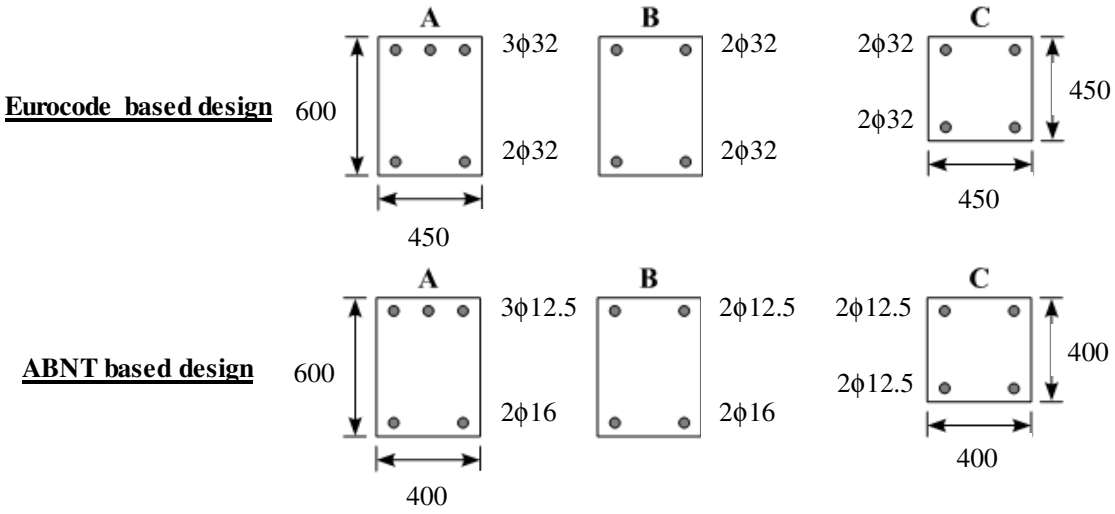

Figure 3: Reinforcement schemes (A, B and C correspond to the sections defined on Fig. 2).

3 FINITE ELEMENT FORMULATION: MULTILAYERED BEAM APPROACH, AND REPRESENTED NONLINEARITIES

The main contribution of this work from a computational point of view is the coupling of the multilayered computation of sectional stresses [5] and the geometrically nonlinear kinematics issued from a corotational Bernoulli beam formulation. This section summarizes the main ingredients of the numerical modeling tool. It presents aspects of the corotational formulation used for introducing nonlinear geometric effects in the multiscale numerical formulation, as well as the adopted material constitutive properties and the governing equations in dynamics.

3.1 Corotational beam kinematics

Geometrical nonlinear effects, as catenary actions, are the result of the interaction of both external and internal forces, and the *deformed shape of a structure*. Works as Batini *et al.* [15] and Souza *et al.* [16] have demonstrated the importance of considering these effects when analyzing composite structures. Dat and Hai [17] have also demonstrated that catenary effects may play an important role on mitigating PC. In this work, the beam's nonlinear kinematics represented by a corotational formulation allows the investigation of possible catenary effects developed in the studied problems.

A corotational formulation, as presented in Crisfield [4] and Batini [18], is a reinterpretation of the deformation of a beam element or, in the most general case, a tridimensional body. This reinterpretation consists in not using the same global reference system in which the structure is inserted for the calculation of strain and displacements of each element but to assume individual local reference systems for these elements instead (Fig. 4), decoupling rigid body rotation from deformation [18].

To implement the corotational formulation it is necessary to define the relation between the displacements in the global (structural) reference system, $\{q_e\}^T = \{u_1 \quad w_1 \quad \theta_1 \quad u_2 \quad w_2 \quad \theta_2\}$, and the ones in the local system, $\{\bar{q}_e\}^T = \{\bar{u} \quad \bar{\theta}_1 \quad \bar{\theta}_2\}$, as defined in Fig. 4. If l_f, l_i and α denote the deformed length, the initial length and the rigid body rotation of the element, respectively, the local kinematic variables are defined by:

$$\begin{bmatrix} \bar{u} \\ \bar{\theta}_1 \\ \bar{\theta}_2 \end{bmatrix} = \begin{bmatrix} l_f - l_i \\ \theta_1 - \alpha \\ \theta_2 - \alpha \end{bmatrix} = \begin{bmatrix} l_f - l_i \\ \theta_1 - \beta - \beta_0 \\ \theta_2 - \beta - \beta_0 \end{bmatrix} \tag{1}$$

where β represents the current angle between the element and the global reference system, and β_0 represents the original value of this angle in the undeformed configuration.

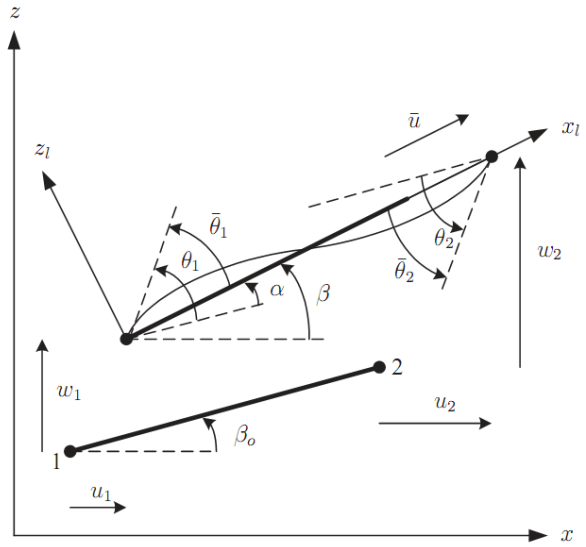

Figure 4: Corotational reference system and kinematic variables [18].

Horizontal displacements are interpolated by using a linear function, while a cubic one is used for vertical displacement of the beam element (Eq. 2). Consequently, axial strain and curvature are calculated through Eq. 3.

$$u = \frac{x}{L}\bar{u}$$
$$w = x\left(1-\frac{x}{L}\right)^2\bar{\theta}_1 + \frac{x^2}{L}\left(\frac{x}{L}-1\right)^2\bar{\theta}_2 \tag{2}$$

Technical information on how the internal force vector and the stiffness matrix of the finite element are derived can be found in [4] and [18].

3.2 Multilayer discretization of an Euler-Bernoulli beam

The formulation deals with a layer discretization of the transversal section for determining stresses in the section of an Euler-Bernoulli beam finite element. Internal forces are obtained from the integration of sectional stresses over three Gauss points along the length of the element.

The discretization of the transversal sections, defined at the Gauss points along the length of the beam, consists of the portioning of the reinforced concrete (composite) section into longitudinal layers (Fig. 5). Note that this produces a multilevel nature that links the dynamic equilibrium on the structural level to the sectional level.

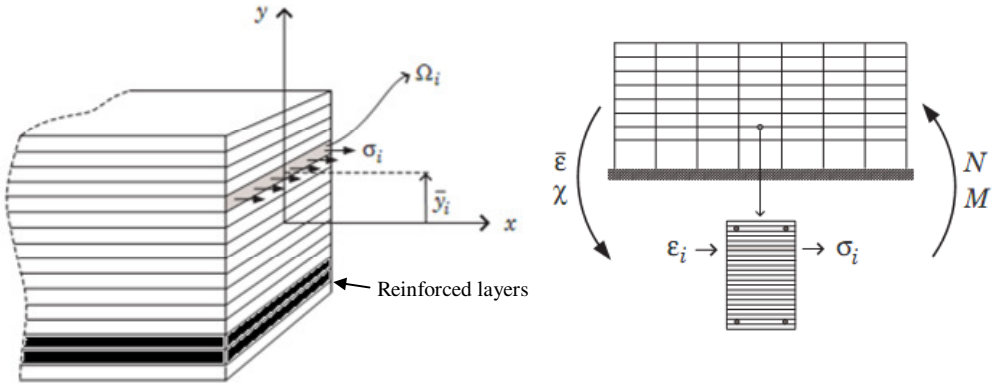

Figure 5: Multilayer discretization of a beam section and shceme of the multiscale framework [5].

The average axial strain and beam curvature computed at an integration point (Eq. 3) are used to obtain the layer total (axial) strain (Eq. 4).

$$\epsilon = \frac{\partial u}{\partial x} = \frac{\bar{u}}{L}$$
$$\chi = \frac{\partial^2 w}{\partial x^2} = \left(-\frac{4}{L}+\frac{6}{L^2}x\right)\bar{\theta}_1 + \left(-\frac{2}{L}+\frac{6}{L^2}x\right)\bar{\theta}_2 \tag{3}$$

$$\epsilon_i = \bar{\epsilon} - \bar{y}_i\chi \tag{4}$$

where,for each layer *i,* at an integration point $\bar{\epsilon}$ is the beam axial strain, $\bar{y}_i$ is the position of layer's center of mass in reference to the section's neutral axis, χ is the beam curvature and ϵ_i is the total strain.

Then, using the nonlinear constitutive relationships for concrete and steel, it is possible to determine the one-dimensional stress acting in each layer (σ_i). At each integration point, the section's generalized stresses are obtained using:

$$\begin{bmatrix} N \\ M \end{bmatrix} = \begin{bmatrix} \sum \sigma_i \Omega_i \\ -\sum \sigma_i \overline{y}_i \Omega_i \end{bmatrix} \tag{5}$$

where σ_i is the one-dimensional stress of layer *i,* Ω_i is the cross-sectional area of the layer and $\begin{bmatrix} N & M \end{bmatrix}^T$ is the vector of generalized stresses ($\sum^{gen}$).

Together with the generalized stresses, the matrix $[B]$ composed of the derivatives of the interpolation functions is used to obtain the internal force vector, as follows:

$$\left\{ f_e^{\text{int}} \right\}^T = \left\{ f_1^x \quad f_1^y \quad c_1 \quad f_2^x \quad f_2^y \quad c_2 \right\} = \int_{V_e} [B]^T \left\{ \sum^{gen} \right\} dV \tag{6}$$

One of the main advantages of this approach is that it makes possible the physical representation of the reinforcements within the cross-section. Another advantage is the inclusion of a gradual sectional degradation effect, consequence of progressive layer failure considering nonlinear constitutive relationships (see Sect. 3.3). Figure 6 exemplifies the stress pattern on the sectional level of an element. The use of a post processing tool allows the identification of the level of stress in each layer and the state of the layer (e.g. elastic/plastic/failed) by using different colors.

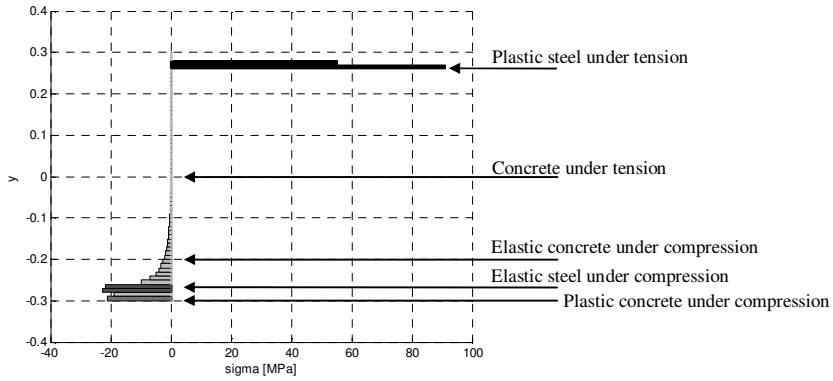

Figure 6: Example of layer stress and layer state plot for a given beam section.

3.3 Constitutive models for concrete and steel

According to Eurocode [2] and ABNT - NBR 6118 [3], class C30 concrete and S500 steel, and C20 concrete and CA50 steel were used for the structural designs, respectively. The constitutive model for these materials is described through a bilinear approximation of the stress-strain behavior as presented below.

a) Concrete

The modeling of concrete behavior was based on recommendations established by [2], [1] and [19], and is depicted on Fig.7. The following assumptions were made for defining this simplified model:

- although concrete develops moderate stresses when working under tension, any structural strength due to this kind of loading is not taken into account, i.e. once concrete is under tension it is considered to be fully cracked and stresses are neglected;
- strains and stresses are proportional during the elastic regime as recommended by [2], instead of the nonlinear curve proposed by [1] and [19]. Young's moduli were set as 32 GPa for C30 and 25 GPa for C20 concrete, respectively;
- for quasi-static loading conditions, the plastic regime is represented by a plateau on the level of 37.9 MPa for C30 concrete and 20 MPa for C20 concrete (Fig. 7);
- the maximum strain under compression in both types of concrete is defined as 0.35%, after which any increase in the strain level will immediately decrease the stress to zero and keeps it at this level in the subsequent loading steps. In this work, this assumption associated with the multilayer discretization allows the investigation of material degradation due to concrete failure (crushing).

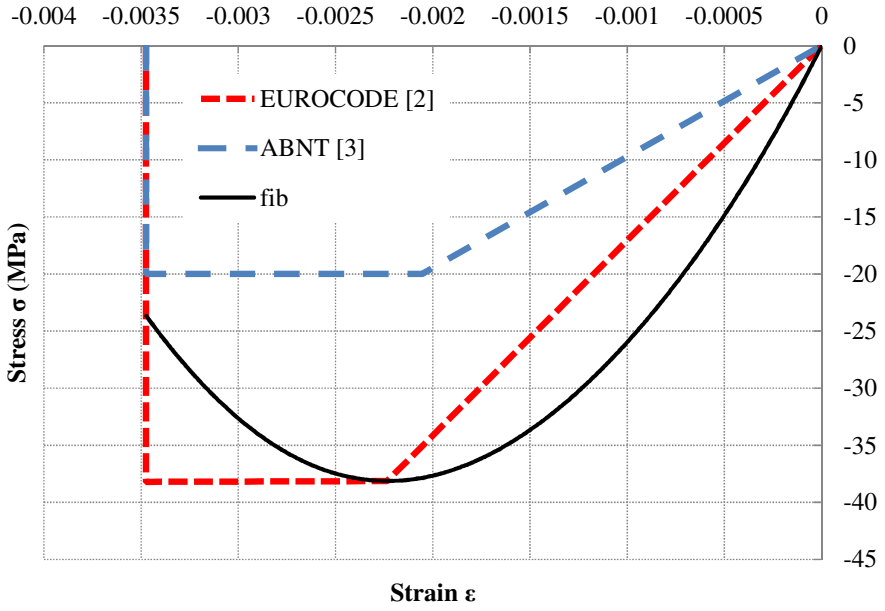

Figure 7: Constitutive model – concrete in compression for quasi-static loading.

b) Steel

According to [2] and [3], the bilinear curve on Fig. 8 represents the correlation between stress and strain for steel under quasi-static loading conditions. The following additional information can also be related to the constitutive behavior of S500 steel and CA50 steel:

- the steel behavior in tension is analogous to the one in compression;
- the steel Young's modulus in the elastic regime, yield stress and ultimate strain are equal to 200 GPa, 500 MPa and 4%;
- just as it was assumed for concrete, stresses in the layers vanish as the strain reaches values larger than 4%, representing steel fracture;
- the ratio between ultimate stress and yield stress is equal to 1.06 [5].

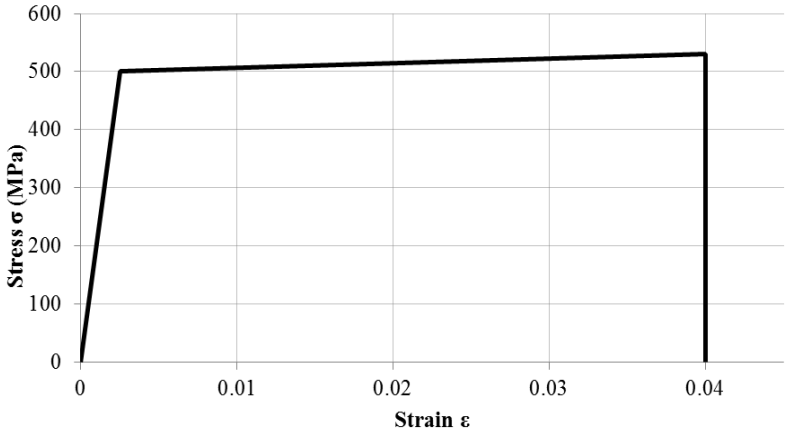

Figure 8: Constitutive model – steel for quasi-static loading

In order to account for the strength enhancement provided by the strain rate dependence of both steel and concrete material behavior [20 - 21], the constitutive models defined above are extended by a strain rate dependent material behavior. The Young's modulus of concrete is set as dependent on the strain rate [5].

To include the strain rate effects in the irreversible behaviour of concrete and steel, a Perzyna type of viscoplastic model is used [22], introducing viscous terms in the constitutive laws. The viscoplatic strain rate used in [5] and that was also used in the present work is a function of the overstress (f) value and is given as follows:

$$\dot{\epsilon}^{vp} = \frac{1}{\eta}\left\langle \frac{f}{\bar{\sigma}_0} \right\rangle^N \frac{df}{d\sigma} \tag{7}$$

where

$\dot{\epsilon}_{vp}$ = viscoplastic strain rate;

η = viscosity parameter, also dependent on the strain rate [5];

$f = (\sigma - \bar{\sigma})$, yield function that accounts for the overstress;

$N = 1$, viscosity parameter [5];

$\bar{\sigma}_0$ = initial one-dimensional yield stress;

σ = one-dimensional stress;

$\bar{\sigma}$ = current one-dimensional yield stress;

$\langle\ \rangle$ = MacAulay brackets;

3.4 Governing equations in dynamics

Equilibrium in dynamics is represented by the equation below, on which an implicit Newmark integration scheme is applied. Note that no artificial/numerical damping is introduced in the system of equations.

$$\left\{f^{\text{int}}(\{q\},\{\dot{q}\})\right\} + [M]\{\ddot{q}\} = \left\{f^{ext}\right\} \tag{8}$$

where $\left\{f^{\text{int}}\right\}$ represents the internal force vector, dependent on the displacement $\{q\}$ and displacements rates, $[M]$ represents the mass matrix and $\left\{f^{ext}\right\}$ is the external force vector.

Since the internal forces are strain rate dependent, their variation with respect to the displacements, i.e. the structural tangent operator, will also be dependent on those rates and include a viscous damping term (Eq. 9).

$$[K_T^*] = \frac{\partial\left\{f^{\text{int}}(\{q\},\{\dot{q}\})\right\}}{\partial\{q\}} = \left.\frac{\partial\left\{f^{\text{int}}(\{q\},\{\dot{q}\})\right\}}{\partial\{q\}}\right|_{\{\dot{q}\}=cte.} + \left.\frac{\partial\left\{f^{\text{int}}(\{q\},\{\dot{q}\})\right\}}{\partial\{\dot{q}\}}\right|_{\{q\}=cte.} \frac{\partial\{\dot{q}\}}{\partial\{q\}} \tag{9}$$

The second term of (Eq. 9) refers to the viscous damping matrix and introduces damping on the structural level *due to the strain rate dependent (viscoplastic) stress-strain relationships* assumed for the materials.

It is noteworthy that the mass matrix of the beam elements was calculated considering the undeformed shape of the structure and kept constant along the whole analysis in this work. Updating the mass matrix as a function of the displacements of the structure is part of future work [23].

4 ASSUMPTIONS CONCERNING THE NUMERICAL SIMULATION AND SIMULATION RESULTS

To prevent the influence of dynamic effects in the initial loading phase, the structure self-weight and service loads are applied in a large period of time, defined as 1000 s. The sudden removal of the column happens subsequently to this loading process. Column removal is modeled as the decrease of the reaction forces, equivalent to the presence of the column, applied at point E (Fig. 9) in a short period of time (0.01 s). The response of the structure is analyzed for a period of two seconds after column removal.

Each model was discretized into approximately 900 elements. Preliminary studies showed that a number between 40 and 60 layers was appropriate for discretizing the cross-sections of the structural elements, i.e. not too many that would make the analysis unaffordable or too few that would introduce significant errors in the obtained results. Thus, 40 layers were used for the discretization of the columns and 60 for the beams.

Besides the point of column removal (E), other reference points were defined for measuring displacements and stresses during the analysis. These points are shown in Fig. 9. The following nomenclature will be used in this section:

EUCO – Eurocode based model, analysed via corotational formulation;
BRCO – ABNT - NBR 6118 based model, analysed via corotational formulation.

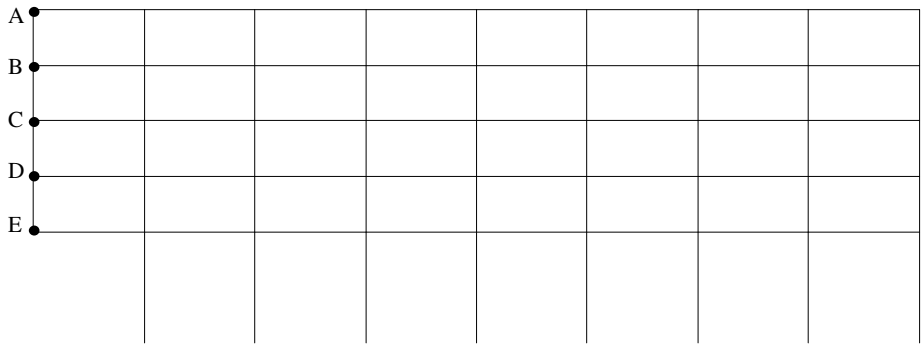

Figure 9: Reference points.

When comparing the final deformed configuration of the EUCO and BRCO models (Figs. 10 and 11), it is clear that the former presents smaller displacements. As shown in Tab. [2], the vertical displacements of BRCO on the reference points are approximately 2.15 times larger than the ones of EUCO. This difference can be associated to the larger sections of the structural elements, to the larger quantity of reinforcement, and to the different material behavior adopted for concrete in the two simulations (Fig. 7). However, it is important to highlight that *both structures were able to overcome the loss of the column and did not initiate the progressive collapse mechanism according to the simulation.*

An additional analysis, using a linear geometric formulation, resulted in displacements 2-3% smaller for both EUCO and BRCO cases. This is believed to be related to the corner position of the removed column that does not benefit from positive catenary effects. However, these effects may play a more important role if an internal column was removed, which can be verified in a future work.

	EUCO	**BRCO**	$V2/V1$
REF. Point	**V1**	**V2**	
A	-0.11700	-0.25007	2.14
B	-0.11924	-0.25523	2.14
C	-0.12134	-0.26021	2.14
D	-0.12349	-0.26525	2.15
E	-0.12645	-0.27208	2.15

Table 2: Vertical displacements at reference points.

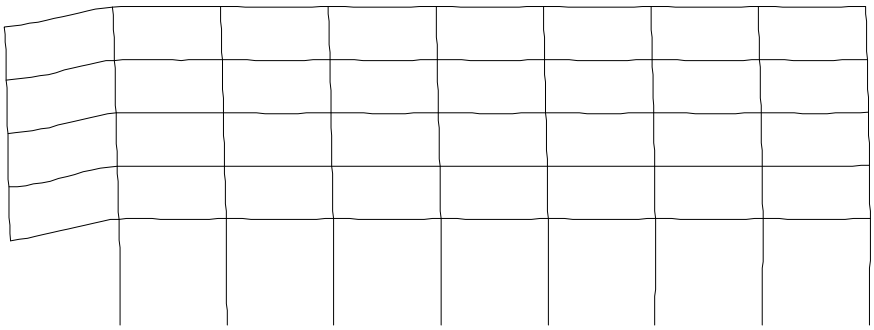

Figure 10: EUCO's deformed configuration (displacements multiplied by 10).

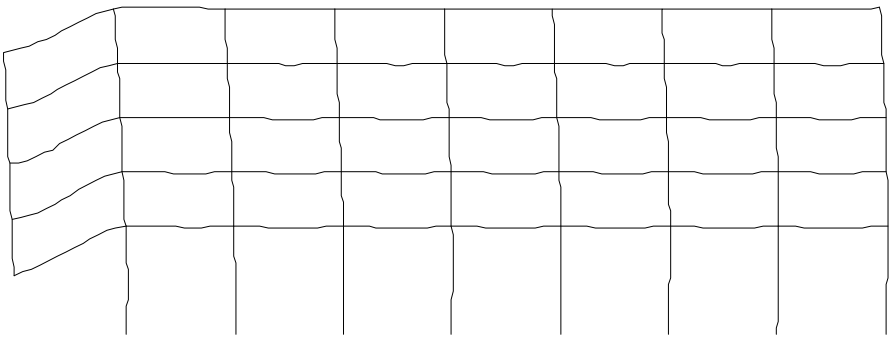

Figure 11: BRCO's deformed configuration (displacements multiplied by 10).

The variation of the vertical displacement of reference point E, after the removal of the column, is represented in Fig. 12 and indicates that although BRCO presents larger displacements, it stabilizes faster than EUCO. The mean displacement value is of approximately 12 cm for EUCO and 25 cm for BRCO. The oscillation observed for the beam's extremity introduces cyclic changes in the pattern of the loading of the structural elements, i.e. repeated reversal of bending moments.

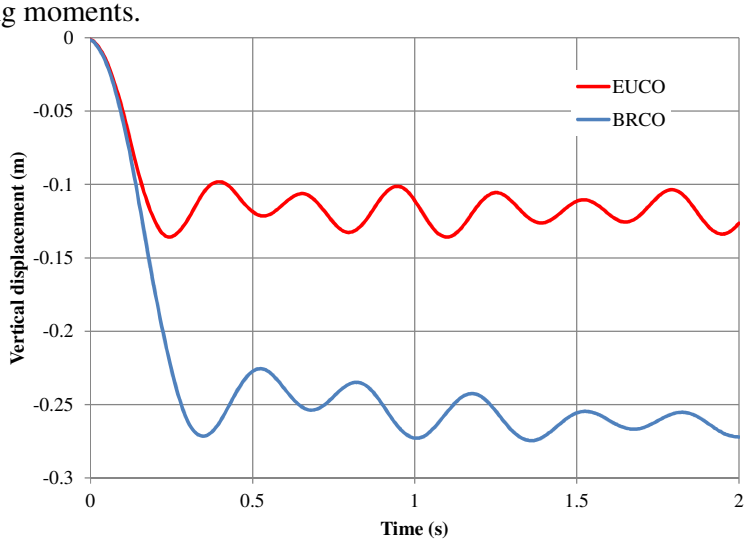

Figure 12: Time variation of vertical displacement at reference point E.

Figures (13) and (14) show that, in terms of plasticity distribution, the effects of the column removal spreads to the whole structure in the BRCO case. For the EUCO case, these effects can barely be identified on other beams than the ones above the removed column. The symbol (•) was used to represent sections in which steel has reached the plastic level and (∇) represents those in which concrete was crushed in less than 30% of the layers. Reinforcement bars did not fail in any of the models, consequently the structures withheld the column removal. It is important to point out that, for EUCO, only the floors immediately above the removed column were affected, which can diminish losses and make it easier to repair the remaining structure.

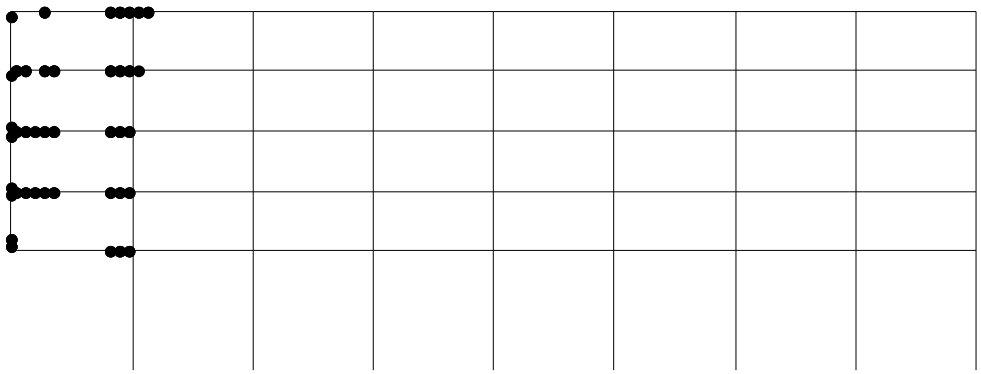

Figure 13: Plasticity distribution at the end of the analysis (EUCO, 2 s after column removal).

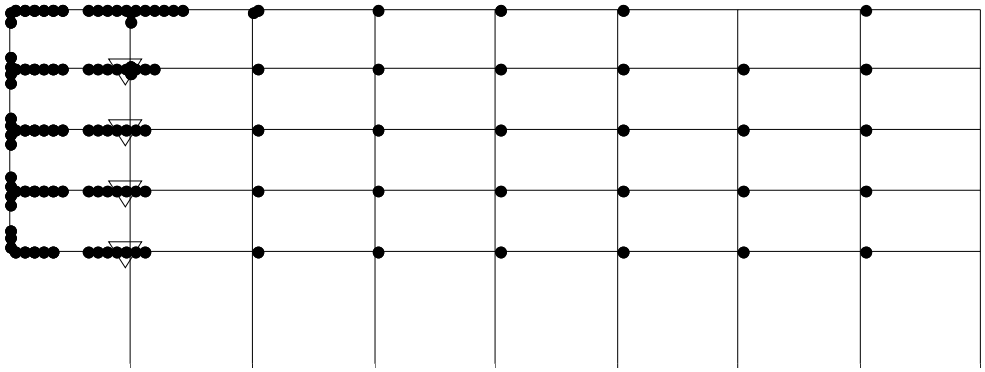

Figure 14: Plasticity distribution at the end of the analysis (BRCO, 2 s after column removal).

5 CONCLUDING REMARKS

This work presents a first attempt to combine dynamic effects, material and geometrical nonlinearities, and sectional degradation through a multilevel approach using a multilayer formulation for the numerical investigation of progressive collapse. Its main focus was to compare two structures, designed in accordance to the minimum requirements of two different building codes, from Europe and from Brazil. Details on the design and assumptions made during the design process were provided, as well as a summary of the applied numerical formulation and the material constitutive behavior.

The slenderer Brazilian structure presented larger displacements and the removal of the column affected the whole structure, in a distributed way. Although none of the structures triggered the progressive collapse mechanism, these results point to a better performance of the European design process, in which only the floors immediately above the removed column were affected.

Future research includes the updating of the structure mass matrix as a function of its deformation, the utilization of constitutive laws that couple plasticity and damage (elastic stiffness degradation), the use of a formulation including shear effects, and the refining of the structural input data, as for example, representing variations of the element's cross-sectional area along the its length.

ACKNOWLEDGMENTS

The authors would like to thank CAPES, CNPq, FAPEMIG, FNRS, Fundação Gorceix and PROPEC for the financial support, and Eng. Everton Batelo, for helping with the structural design of the ABNT - NBR 6118 based structure.

REFERENCES

[1] International Federation for Structural Concrete (fib), *Constitutive modelling of high strength/high performance concrete, State-of-art report*, fib Bulletin **42**, 2008.

[2] EN 1992-1-1, *Eurocode 2: Design of concrete structures - Part 1-1: General rules and rules for buildings*, December, 2004.

[3] ABNT - Associação Brasileira de Normas Técnicas, *NBR 6118: projeto de estruturas de concreto: procedimento*, Rio de Janeiro, 2003.

[4] Crisfield, M. A., *Non-Linear Finite Element Analysis of Solids and Structures, Vol. **I**.* John Wiley & Sons, 1997.

[5] Iribarren, B. S., Berke, P., Bouillard, Ph., Vantomme, J., Massart, T.J., Investigation of the influence of design and material parameters in the progressive collapse analysis of RC structures, *Engineering Structures*, Vol. **33**, 2805-2820, 2011.

[6] Marjanishvili, S., Agnew, E., Comparison of various procedures for progressive collapse analysis, *Journal of Performance of Constructed Facilities*, *Vol. **20***, 2006.

[7] TsaiM-H, Lin B-H., Investigation of progressive collapse resistance and inelastic response for an earthquake-resistant RC building subjected to column failure, *Engineering Structures*, Vol. **30**, 3619–28, 2008.

[8] Kim H-S, Kim J, An D-W., Development of integrated system for progressive collapse analysis of building structures considering dynamic effects, *Advances in Engineering Softwares*, Vol. **40**, 1–8, 2009.

[9] Kwasniewski, L., Nonlinear dynamic simulations of progressive collapse for a multistore building, *Engineering Structures*, Vol. **32**, 1223–35, 2010.

[10] United States General Services Administration (GSA), *Progressive collapse analysis and design guidelines for new federal office buildings and major modernization projects,* Washington DC, 2003.

[11] Izzuddin, B. A., Robustness by design – Simplified progressive collapse assessment of building structures, *Stahlbau*, Vol. **79**, 556–564, 2010.

[12] Khandelwal K., El-Tawil S., Pushdown resistance as a measure of robustness in progressive collapse analysis, *Engineering Structures*, Vol. **33**, 2653-2661, 2011.

[13] Buildsoft NV, *Diamonds 2010 r.01,* http://www.buildsoft.eu (Last access: 07/03/2013).

[14] Cype, Cypecad 2011, http://www.cype.pt/ (Last access: 07/03/2013).

[15] Battini, J-M., Nguyen, Q-H., Hjiaj, M., Non-linear finite element analysis of composite beams with interlayer slips, *Computer and Structures*, Vol. **87**, 904-912, 2009.

[16] Sousa Jr., J. B. M., Oliveira, C. E. M., Silva A. R., Displacement-based nonlinear finite element analysis of composite beam columns with partial interaction, *Journal of Constructional Steel Research*, Vol. **66**, 772 -779, 2010.

[17] Tan, K. H., & Pham, X. D., Membrane actions of RC slabs in mitigating progressive collapse of building structures. *Proceedings of the Design and Analysis of Protective Structures*, Singapore, 2010.

[18] Battini, J-M., *Corotational beam elements in instability problems*, Ph.D Thesis, Royal Institute of Tecnology, Department of Mechanics, Stockholm, Sweden.

[19] International Federation for Structural Concrete (fib), *Practitioners' guide to finite element modelling of reinforced concrete structures. State-of-art report*, fib Bulletin **45**, 2008.

[20] Malvar, L. J, Crawford, J. E., *Dynamic increase factors for concrete*, 28th DDESB seminar, Orlando, FL, USA, 1998.

[21] Bischoff, P. H, Perry, S. H., Compressive behaviour of concrete at high strain rates, *Materials and Structures*, Vol. **24**, 425–50, 1991.

[22] Heeres O. M., Suiker A. S. J., de Borst R., A comparison between the Perzyna visco-plasticmodel and the Consistency viscoplastic model, *European Journal of Mechanics A/Solids*, Vol. **21**, 1–12, 2002.

[23] Le, T-N, Battini, J-M, Hjiaj, M., Efficient formulation for dynamics of corotational 2D beams, *Computational Mechanics*, Vol. **48**, 153-161, 2011.